Confronting the Food-Energy-Environment Trilemma: Global Land Use in the Long Run*

Jevgenijs Steinbuks† and Thomas W. Hertel‡

June 6, 2012

Abstract

This study analyzes the optimal allocation of the world's land resources over the course of the next century within a dynamic forward-looking framework, which brings together distinct strands of economic, agronomic, and biophysical literature and incorporates key drivers affecting global land-use. We show that, while some deforestation is optimal in the near term, the desirability of further deforestation is eliminated by mid-century under the baseline scenario. While adverse productivity shocks from climate change have a modest effect on global land use, when combined with high growth in energy prices this leads to significant deforestation and higher GHG emissions than in the baseline. Imposition of a GHG emissions constraint further heightens the competition for land, as fertilizer use declines and land-based mitigation strategies expand. However, the effectiveness of such a pre-announced constraint is largely diluted by inter-temporal substitution of deforestation which accelerates prior to imposition of the target.

JEL: C61, Q15, Q23, Q26, Q40, Q54

Keywords: biofuels, climate change, deforestation, energy, environment, food, forestry, forest vintages, GHG emissions, global land use

*Acknowledgements: We would like to thank Ujjayant Chakravorty, Kenneth Judd, Todd Munson, Paul Preckel, Brent Sohngen, and the participants of the 4th International Workshop on Empirical Methods in Energy Economics, the American Geophysical Union Annual Meetings, the American Economic Association Annual Meetings, and research seminar at Purdue University for their helpful suggestions and comments. We appreciate the financial support from the National Science Foundation, grant 0951576 "DMUU: Center for Robust Decision Making on Climate and Energy Policy".

†Center for Global Trade Analysis, Purdue University and Center for Robust Decision Making on Climate and Energy Policy, University of Chicago.

‡Department of Agricultural Economics and Center for Global Trade Analysis, Purdue University.

1 Introduction

The allocation of the world's land resources over the course of the next century has become a pressing research question. Continuing population increases, improving, land-intensive diets amongst the poorest populations in the world, increasing production of biofuels and rapid urbanization in developing countries are all competing for land even as the world looks to land resources to supply more environmental services. The latter include biodiversity and natural lands, as well as forests and grasslands devoted to carbon sequestration. And all of this is taking place in the context of faster than expected climate change which is altering the biophysical environment for land-related activities. This combination of intense competition for land, coupled with highly uncertain future productivities and valuations of environmental services, gives rise to a significant problem of decision-making under uncertainty. The issue is compounded by the inherent irreversibility of many land use decisions.

The goal of this paper is to determine the optimal profile for global land use in the context of growing commercial demands for food and forest products, increasing non-market demands for ecosystem services, and more stringent GHG mitigation targets. Our research is related to a number of studies, analyzing particular aspects of land-use decisions. The bulk of the literature on agriculture and land-use studies how the agricultural system adapts to rising food demand stemming from income and population growth, as well as to changes in agricultural productivity of commercial land (Ianchovichina et al. 2001, Golub et al. 2009, Choi et al. 2011b). The literature on renewable energy and land-use focuses heavily on the competition for land between biofuels and food production, and the ensuing implications for land-based GHG emissions (Gurgel et al. 2007, Chakravorty et al. 2008, Gillingham et al. 2008, Searchinger et al. 2008, Chakravorty et al. 2011, Chen et al. 2011). The literature on commercial forestry and land-use studies the allocation of land to the commercial forestry sector in the context of timber production and climate mitigation policies (Stavins 1999, Sohngen and Mendelsohn 2003, Richards and Stokes 2004, Sohngen and Mendelsohn 2007, Choi et al. 2011a). The literature on ecosystem services and land-use studies optimal natural land conservation decisions taking into account irreversibility in disruption of biodiversity and significant option values attached to the future stream of benefits from ecosystem services (Conrad 1997, Conrad 2000, Bulte et al. 2002, Leroux et al. 2009).[1]

[1] Recent studies by Antoine et al. (2008) and Gurgel et al. (2011) attempted to integrate the

Finally, the literature on GHG Sequestration and land-use explores different strategies to manage anthropogenic carbon emissions from terrestrial systems, and their implications for land-use. (Wise et al. 2009, Burney et al. 2010).

The model which we develop seeks to integrate these five, rather distinct strands of literature into a single, intertemporally consistent, analytical framework, at global scale. Our analysis is based on a dynamic long-run, forward-looking partial equilibrium framework, in which the societal objective function places value on food production, liquid fuels (including biofuels), timber production, forest carbon and biodiversity. A non-homothetic AIDADS utility function represents model preferences, and, as society becomes wealthier, places greater value on eco-system services, and smaller value on additional consumption of food, energy and timber products. Given the importance of land-based emissions to any GHG mitigation strategy, as well as the potential impacts of climate change itself on the productivity of land in agriculture, forestry and ecosystem services, we aim to identify the optimal allocation of the world's land resources, over the course of the next century, in the face of alternative GHG constraints. The forestry sector is characterized by multiple forest vintages, which add considerable computational complexity in the context of this dynamic forward-looking analysis.[2]

We solve the model over the 200 year period: 2005- 2204, focusing analysis on the next century. Our baseline accurately reflects developments in global land use over the years that have already transpired, while also incorporating projections of population, income and demand growth from a variety of recognized sources. Though we do not explicitly incorporate uncertainty at the optimization stage of the model, we examine the ways in which global land-use responds to changes in factors corresponding to the most important sources of uncertainty associated with this problem. Specifically, we consider three counterfactual scenarios: higher growth in energy prices, lower growth in agricultural productivity due to higher temperatures, and global GHG emissions regulations.

We show in our model baseline that, in the absence of market imperfections,

---

demand for recreation services into a broader land-use perspective using recursive-dynamic multi-regional CGE model of the world economy (MIT-EPPA).

[2]Because of their complexity most of the models employed to analyze land-use decisions at broad scale are solved recursively rather than as fully inter-temporal forward-looking optimization problems. The forward-looking approach adopted in our paper is less common, notwithstanding its better capabilities to address important economic policy issues such as inter-temporal allocation of GHG emission flows from land-use through abatement policies, efficiency implications of carbon taxes and caps, and endogenous depletion of non-renewable land resources. For a detailed discussion on relative pros and cons of recursive versus forward-looking approaches in climate policy analysis, see Babiker et al. (2009).

deforestation associated with cropland expansion, which accounts for a large share of land-use GHG emission, should optimally decline in the medium run. Though adverse productivity shocks from climate change have a modest effect on global land use, it does lead to significant declines in consumption of agricultural output over the long-run. Energy prices and policies have a strong effect on the overall amount of land used in agriculture. In a 'perfect storm' of high growth in energy prices and declining agricultural productivity growth, additional demand for cropland leads to significant deforestation and higher GHG emissions than in the baseline. The introduction of GHG emissions constraint leads to a significant long-run reduction in GHG emission flows. However, an even greater increase in GHG emissions before the constraint is introduced makes it ineffective over the hundred year term, thereby confirming the 'green paradox' (Sinn 2008).

2 Model Outline

The model which we develop seeks to integrate these five, rather distinct strands of literature into a single, intertemporally consistent, analytical framework, at global scale. It is a deterministic, discrete dynamic, finite horizon partial equilibrium model. Income, population, wages, oil prices, total factor productivity, and other variable input prices are assumed to be exogenous. The model focuses on the optimal allocation of scarce land across competing uses across time.

There are two natural resources in the model: land and fossil fuels. The supply price of fossil fuels is predetermined, and is expected to rise over time. The supply of land is fixed and faces competing uses that are determined endogenously by the model.

We analyze eight sectors producing intermediate and final goods and services. The agrochemical sector converts fossil fuels into fertilizers that are used to boost yields in the agricultural sector. The agricultural sector combines cropland and fertilizers to produce intermediate output that can be used to produce food or biofuels. The food processing sector converts agricultural output into food products that are used to meet the global food demand. The biofuels sector converts agricultural products into liquid fuels, which substitute imperfectly for fossil fuels in final demand. The energy sector combines fossil fuels with the biofuels, and the resulting mix is further combusted to satisfy the demand for energy services. The forestry sector produces an intermediate product, which is further used in timber processing. The timber processing sector converts output from the forestry sector into a final timber product, which satisfies commercial demands for lumber and other articles of wood. The recreation sector provides a public good to society in the form of ecosystem services. The production of other goods and services are predetermined.

The societal objective function being maximized places value on processed food, energy services, timber products, and eco-system services. Emissions of greenhouse gases (GHGs) are central to the problem at hand. These are currently treated as a time-varying constraint on the flow of GHGs (emissions target). As the model focuses on the representative agent's behavior, the resource endowments and consumption products are expressed in per-capita terms. The model's structure, equations, variables, and parameters are summarized in technical appendix.

2.1 Resource Use

2.1.1 Land

The total land endowment in the model, $\overline{\Lambda}$, is fixed, so that the per-capita land endowment, Λ_t, declines with increases in population. The land in the economy comprises of natural forest lands – which are in an undisturbed state (e.g., parts of the Amazon), N_t, and commercial lands, L_t, both of which are expressed in per capita terms. The per-capita land endowment constraint is

$$\Lambda_t = \frac{\overline{\Lambda}}{\Pi_t} = N_t + L_t, \tag{1}$$

where Π_t is the predetermined population at time t. Based on the previous literature on natural land use (Antoine et al. 2008, Gurgel et al. 2011) we assume that the natural land consists of two types. Institutionally protected land, N^R, includes natural parks, biodiversity reserves and other types of protected forests. This land is used to produce ecosystem services for society, and cannot be converted to commercial land. Unmanaged natural land, N^N, can be accessed and either converted to commercial land (deforested) or to protected land. Once the natural land is deforested, its potential to yield ecosystem services is interrupted and cannot be restored within the (single century) time frame of the analysis. Thus, the conversion of natural lands for commercial use is an irreversible decision. Equations describing allocation of commercial land across time and different uses are as follows, where lower case variables describe flows and upper cases correspond to stocks, and all variables are expressed on a per capita basis:

$$N_t = N_t^N + N_t^R. \tag{2}$$

$$N_{t+1}^N = N_t^N - \Delta L_t - \Delta N_t^R,\ N_0^N > 0, \tag{3}$$

and

$$N_{t+1}^R = N_t^R + \Delta N_t^R,\ N_0^R > 0, \tag{4}$$

Equation (2) shows that the total endowment of natural land is a sum of the hectares of reserved and non-reserved natural land. Equation (3) shows that at each period of time the area of unmanaged natural land with initial stock, N_0, declines by the amounts allocated for conversion to commercial and protected land, ΔL_t and ΔN_t^R, where Δ operator denotes a change in variables L_t and N_t^R. Equation (4) shows that at each period of time, the total area of reserved land with initial stock of N_0^R increases by the amount of newly protected land, ΔN_t^R.

Accessing the natural lands comes at cost, c_t^N, associated with building roads and other infrastructure (Golub et al. 2009). In addition, converting natural land to reserved land entails additional costs, c_t^R, associated with passing legislation to create new natural parks. We assume that these costs are continuous, monotonically increasing, and strictly convex functions of the share of natural land previously accessed. There are no additional costs of natural land conversion to commercial land, as these costs are offset by the revenues from deforestation.

Commercial lands are used in either the agriculture or forestry sectors (we ignore residential, retail, and industrial uses of land in this partial equilibrium model of agriculture and forestry). Equations describing allocation of commercial land across time and between agriculture and forestry are:

$$L_t = G_t + W_t. \tag{5}$$

and

$$L_{t+1} = L_t + \Delta L_t,\ L_0 > 0. \tag{6}$$

Equation (5) shows that total endowment of commercial land, L, is a sum of the hectares of commercial land dedicated to agriculture, G, and managed forest, W, respectively. Equation (6) shows that at each period of time, the total area of commercial land with initial stock of L_0 increases by the amount of converted non-reserved natural land, ΔL.

2.1.2 Fossil Fuels

The fossil fuels, x, have two competing uses in our partial equilibrium model of land-use. A fraction of fossil fuels, x^{ϕ}, is converted to fertilizers that are further used in the agricultural sector. The remaining amount of fossil fuels, x^e, is combusted to satisfy the demand for energy services. The total supply of fossil fuels is thus given by

$$x_t = x_t^{\phi} + x_t^e. \tag{7}$$

The cost of fossil fuels, c_t^x, is pre-determined, and reflects the expenditures on fossil fuels' extraction, transportation and distribution, as well the costs associated with GHG emissions control (e.g. carbon prices) in the non-land-based economy.

2.2 Agrochemical Sector

The agrochemical sector consumes an amount of fossil fuels, denoted by x^{ϕ}, and converts them into fertilizers that are further used in the agricultural sector. The production of fertilizers, ϕ, is a simple engineering process that can be described by a linear production function:

$$\phi_t = \theta^{\phi} x_t^{\phi}, \tag{8}$$

where θ^{ϕ} is the rate of conversion of fossil fuels to fertilizers. We assume that the non-energy cost of conversion of fossil fuels to fertilizers, c^{ϕ}, is constant and scale-invariant.

2.3 Agricultural Sector

The agricultural sector combines the agricultural land and fertilizers to deliver an output, g, that can be either converted to food, f, or biofuels, b. Agricultural land and fertilizers are imperfect substitutes in the production of agricultural products. The output of the agricultural product, g, is thus determined by the constant elasticity of substitution (CES) function:

$$g_t = \theta_t^g \left[\alpha^g \left(G_t\right)^{\rho_g} + \left(1-\alpha^g\right)\left(\phi_t\right)^{\rho_g}\right]^{\frac{1}{\rho_g}}, \tag{9}$$

where θ_t^g and α^g are, respectively, the yield of agricultural land and the value share of land in production of agricultural product at the benchmark time 0. The parameter $\rho_g = \frac{\sigma_g - 1}{\sigma_g}$ is a CES function parameter proportional to the elasticity of substitution of agricultural land for fertilizers, σ^g. The production of agricultural output is also subject to additional costs from use of other production factors (such as e.g. labor or capital), the prices of which are predetermined in our partial equilibrium model. We assume that those costs per ton of agricultural product, c^g, are exogenous and scale-invariant.

2.4 Food Processing Sector

The food processing sector converts an amount of agricultural product, g, into food products and services, f, that are further consumed in final demand. The purpose of this sector in the model is to capture the efficiency gains from technology improvements in food production, which result in lower requirements for agricultural inputs in final demand.[3] The conversion process is represented by the following production function:

$$f_t = \theta_t^f g_t, \tag{10}$$

where θ_t^f is the total factor productivity (TFP) of the food processing sector, which captures the technological progress in both direct transformation of agricultural product into edible food, and the storage, transportation, and distribution of processed food. We assume that the food processing costs per ton of food products, c^f, are exogenous and scale-invariant.

2.5 Biofuels Sector

The biofuels sector consumes the remaining amount of agricultural product to produce biofuels, b. We assume that a ton of agricultural product, g, can be

[3]For example, technological innovation in food conservation results in fewer losses from spoilage, and, correspondingly, lower amounts of processed food needed to satisfy the commercial demand for food. Correspondingly, input requirements for agricultural product also decrease.

converted to θ^b tons of oil equivalent ($toe's$) of biofuels. The output of biofuels is thus given by

$$b_t = \theta^b \left(g_t - \frac{f_t}{\theta^f} \right). \tag{11}$$

The agricultural product's conversion to renewable fuel incurs additional non-food processing cost, c^b. We assume this cost is constant and scale-invariant.[4]

2.6 Energy Sector

The energy sector consumes fossil fuels, x^e, and biofuels, b, that are further combusted to satisfy the demand for energy services. As displacement of fossil fuels by biofuels is limited by technological barriers[5] we assume these fuels are imperfect substitutes. Total production of fuel input, e_t^f, is given by the constant elasticity of substitution (CES) function:

$$e_t^f = \gamma^e \left(\alpha^b \left(b_t \right)^{\rho_b} + \left(1 - \alpha^b \right) \left(x_t^e \right)^{\rho_b} \right)^{\frac{1}{\rho_b}}, \tag{12}$$

where the parameter γ^e describes the technology of energy production, α^b is the value share of biofuels in energy production at the benchmark time 0, and $\rho_b = \frac{\sigma_b - 1}{\sigma_b}$ is a CES function parameter proportional to the elasticity of substitution of fossil fuels for biofuels, σ_b.

The total cost of energy is a sum of the costs of fossil fuels and biofuels net of land-use costs:

$$c_t^e = c^b + c_t^x. \tag{13}$$

We allow for the possibility of efficient use of fuel inputs. One *toe* of energy from fossil fuel or biofuel combusted yield θ_t^e *toe's* of energy services, e :

$$e_t = \theta_t^e e_t^f, \tag{14}$$

where the function θ_t^e reflects the energy efficiency, i.e. the amount of energy services provided by one *toe* of the energy fuel (Sorrell and Dimitropoulos 2008, p. 639).

[4] The biofuels sector is represented by the first-generation biofuels with well established production technology. With introduction of new generation biofuels one would expect these costs to decline, and biofuels conversion rate to increase as the biofuels' production technology improves. We show the model sensitivity to changes in these parameters in technical appendix.

[5] These barriers include different technology requirements for flex fuel vehicles using ethanol and gasoline blends (E85), as well as availability of fuelling stations supplying biofuels.

2.7 Forestry Sector

The forestry sector is characterized by V vintages of forest trees. At the end of period t each hectare of managed forest land, $W_{v,t}$, has an average density of tree vintage age v, with the initial allocation given and denoted by $W_{v,0}$. Each period of time the managed forest land can be either planted, harvested or simply left to mature. The newly planted trees occupy W^p hectares of land, and reach the average age of the first tree vintage next period. The harvested area occupies H_v hectares of forest land. If the managed forest land is harvested, it yields θ_v^w tons of forest product (raw timber), w_v, where θ_v^w is the merchantable timber yield function, which is monotonically increasing in the average tree density of age v. Forest land becomes eligible for harvest when planted trees reach a minimum age for merchantable timber, $\overline{v}$. Managed forest areas with the average density of oldest trees V have the highest yield of θ_V^w . They do not grow further and stay until harvested. In addition, conversion of natural forest land to commercial land (deforestation) yields timber benefits. We assume that natural forest lands are occupied by old trees, so deforested area, ΔL, yields θ_V^w tons of timber.

We assume that the average harvesting costs per ton of forest product, are invariant to scale and are the same across all managed forest areas of different age. With continuous growth up to vintage V, the average long-run cost of harvesting per hectare of managed forest land, c^w, is therefore a declining function of timber output. Harvest of managed forests and conversion of harvested forest land to agricultural land is subject to additional short-run adjustment costs. The average planting costs per hectare of newly forest planted, c^p, are invariant to scale and are the same across all vintages.

The following equations describe the forestry sector:

$$W_t = \sum_{v=1}^{V} W_{v,t}, \tag{15}$$

$$W_{v+1,t+1} = W_{v,t} - H_{v,t}, \;\; v < V-1 \tag{16}$$

$$W_{V,t+1} = \sum_{V-1}^{V} W_{v,t} - H_{v,t} \tag{17}$$

$$W_{1,t+1} = W_t^p, \tag{18}$$

and

$$w_t = \sum_{v=1}^{V-1} \theta^w_{v,t} H_{v,t} + \theta^w_{V,t} \left(H_{V,t} + \Delta L_t\right), \tag{19}$$

Equation (15) describes the composition of managed forest area across forest vintages. Equation (16) illustrates the harvesting dynamics of forest areas with the average ages v and V. Equation (18) shows the transition from planted area, W^p, to new forest vintage area. Equation (19) describes the output of forest product from harvested forest areas of average tree age v and deforested natural lands.

2.8 Timber Processing Sector

The timber processing sector converts harvested forest product, w, into processed timber products, s, that are further consumed in final demand. Similar to food processing, the purpose of this sector in the model is to capture the efficiency gains from technology improvements in timber production, which result in lower requirements for forest products in final demand.[6] The conversion process is represented by a linear production function:

$$s_t = \theta^s_t w_t, \tag{20}$$

where θ^s is the TFP of the timber processing sector, which captures the technological progress in both direct transformation of forest product into processed timber, and the quality improvements and durability of timber products. We assume that the timber processing costs per ton of food products, c^s, are exogenous and scale-invariant.

2.9 Recreation Sector

The recreation sector uses the reserved natural land to produce ecosystem services, such as hunting, fishing, and wildlife viewing. The output for ecosystem services, r_t, is given by

$$r_t = \theta^r_t N^R_t, \tag{21}$$

[6] For example, technological innovation in durability of timber products results in their less frequent replacement. Therefore lower amounts of forest product are needed to satisfy the commercial demand for timber products.

where θ_t^r is the TFP of the recreation sector. The average cost of producing ecosystem services (expenditures to maintain protected natural lands) per hectare of reserved natural land, c^r, is exogenous and scale-invariant.

2.10 Other Goods and Services

The production of other goods and services, o_t, in this model is predetermined. The reason we include it in this partial equilibrium model is to complete the demand system (described in a section below), which determines welfare. As the supply of other goods and services is predetermined, we assume that they grow at the overall rate of TFP growth, which is equal to the world economy's TFP growth rate[7]. Because the production of other goods and services does not draw on the land resource, we assume without loss of generality that their cost of production is zero.

2.11 GHG Emissions

The GHG emissions flows, z_t, in the model result from a number of sources: (a) the use of fossil fuels, (b) the conversion of unmanaged and managed forests to agricultural land (deforestation), (c) non-CO_2 emissions from use of fertilizers in agricultural production, and (d) net GHG sequestration through forest sinks (which includes the GHG emissions from harvesting forests). We differentiate between the emissions resulting from the use of fossil fuels, z^x, and the emissions resulting from land-use, z^L, because the price path for fossil fuels is pre-determined, whereas the other sources of GHG emissions are endogenous.

We assume that GHG emissions are linearly related to the use of fossil fuels, and the allocations of commercial lands. A *toe* of fossil fuel combusted emits μ^x tons of CO_2 equivalent (tCO_2e). Fertilizer production process emits μ^ϕ tCO_2e per ton of fertilizer produced. A ton of fertilizer applied to agricultural land emits μ^g tCO_2e.

GHG's can also be reduced by carbon forest sequestration. A hectare of forest vintage v sequesters μ_v^w tCO_2e. Young forest vintages grow quickly and sequester carbon at a rapid rate. Older vintages grow slowly and eventually cease to sequester carbon. As the unmanaged forest land (both reserved and non-reserved) comprises mainly the older tree vintages, its potential to sequester additional GHGs is small, and may be ignored. However, the potential

[7] The economy's output has a small fraction of endogenously determined output from land-use. We ignore this complication in this partial-equilibrium model.

for GHG releases when these trees are cut down and burned or left as slash (Fearnside 2000, Houghton 2003) is large. The conversion of natural forest land to commercial land entails emissions of μ^L tCO_2e per hectare of land deforested. Harvesting managed forests results in emissions of $(1-\varphi)\mu_v^h$ tCO_2e per hectare of land harvested, where μ_v^h is the carbon stock associated with harvested tree vintage v, and φ is the share of permanently stored carbon in harvested forest products. We ignore the annual sequestration of carbon by agricultural product, as those crops are either consumed or combusted in the form of bioenergy.

Based on the above, the equations describing net GHG flows in the economy are

$$z_t = z_t^x + z_t^L, \tag{22}$$

$$z_t^x = \mu^x x_t^e + \mu^\phi x_t^\phi, \tag{23}$$

and

$$z_t^L = \mu^L \Delta L_t + \mu^\phi x_t^\phi + (1-\varphi)\sum_{v=1}^{V} \mu_v^h H_{v,t} - \sum_{v=1}^{V} \mu_v^w W_{v,t}. \tag{24}$$

Equation (22) describes the composition of GHG emissions flows. Equation (23) describes the GHG emissions from the use of fossil fuels. Equation (24) shows net GHG emissions from deforestation, agricultural production, and forest sequestration.

Finally, we consider institutional control of GHG emissions' flows (e.g. through the Kyoto Protocol), which foresees their gradual reduction and the stabilization of atmospheric carbon stocks. Specifically, we assume that at any point of time net GHG emissions from deforestation, application of fertilizers, and forest sequestration cannot exceed the emissions' quota, $\overline{z}^L$. We do not impose the emissions' constraints on GHG emissions from fossil fuels' combustion and fertilizers' production because they are exogenously determined. Rather we assume that emissions control instruments are reflected in exogenous fossil fuels' prices, which affect the demand for fossil fuels. Finally, because biofuels provide a renewable alternative to fossil fuels, we credit the emissions' quota, $\overline{z}^L$,by the amount of fossil fuels' emissions displaced by the biofuels.[8] The resulting

[8] This doesn't necessarily mean that biofuels are 'greener' than fossil fuels. That will depend on the emissions associated with agricultural production and natural land conversion.

relationships for emissions control are

$$z_t^L \leq \overline{z}_t^L = \theta_t^z \left(z_t^L - \left(1 - \frac{\mu^b}{\mu^x}\right) b_t \right), \tag{25}$$

where global warming intensity, θ_t^z is a function determining the evolution of the GHG emissions' quota over time, and μ^b are non-land-use emissions of biofuels' production. Equation (25) describes the constraint on non-fossil fuel emissions in the atmosphere, and shows how this constraint is derived.

2.12 Preferences

The representative agent's utility, U, is derived from the consumption of food products, energy services, timber products, ecosystem services and other goods and services. The specific functional form for the utility function in this study is based on implicitly directive additive preferences, AIDADS (Rimmer and Powell 1996). Our choice of the utility function based on AIDADS preferences is motivated by its several important advantages over other functional forms underpinning standard models of consumer demand.[9] First, similar to the well-known AIDS demand system (Deaton and Muellbauer 1980) the AIDADS model is flexible in its treatment of Engel effects, i.e. the model "allows the MBS' (Marginal Budget Shares) to vary as a function of total real expenditures" (Rimmer and Powell 1996, p. 1614). Second, the AIDADS has global regularity properties, in contrast to the local properties of AIDS[10]. This is essential for solution of the model over a wide range of quantities. A number of studies (Cranfield et al. 2003, Yu et al. 2004) demonstrated that AIDADS outperforms other popular models of consumer demand in projecting global food demand, which makes it especially well-suited for the economic modelling of land-use.

The utility function for the AIDADS system is the implicitly directly additive function (Hanoch 1975):

$$\sum_{q=f,e_s,w,r,o} F(q,u) = 1, \tag{26}$$

where $q = \{f, e^s, w, r, o\}$ is the consumption bundle, u is the utility level

[9] The most popular demand systems estimated in recent applied work are the Homothetic Cobb-Douglas System (HCD), the Linear Expenditure System (LES), the Constant Difference of Elasticities Demand System (CDE), and the Almost Ideal Demand System (AIDS).

[10] One of well-known limitations of the AIDS system is that its budget shares fall outside $[0, 1]$ interval. This frequently occurs when AIDS is applied to model the demand for staple food when income growth is large (Yu et al. 2004, p. 102).

obtained from the consumption of goods or services q, and $F(q,u)$ is a twice-diffirentiable monotonic function that is strictly quasi-concave in q. Based on Rimmer and Powell (1996), the functional form for $F(q,u)$ is

$$F(q,u) = \frac{\alpha_q + \beta_q \exp(u)}{1+\exp(u)} \ln\left(\frac{q-\overline{q}}{A\exp(u)}\right). \tag{27}$$

In equation (27) the parameters α_q and β_q define the varying marginal budget shares of goods and services q in the consumers' total real expenditures. The parameter $\overline{q}$ defines the subsistence level of consumption of goods and services q. The functional form of $F(q,u)$ implies that the consumption of goods and services q is always greater than their subsistence levels, $\overline{q}$. The parameter A affects the curvature of the transformation function $F(q,u)$. The AIDADS system imposes standard non-negativity and adding-up restrictions based on the economic theory. These restrictions ensure that the consumers' marginal budget shares and minimal consumption level of goods and services $\overline{q}$ are greater or equal to zero, and the sum of marginal budget shares in total real expenditures does not exceed one.

Rimmer and Powell (1996, p. 1615) demonstrate that maximizing the utility function (26) subject to the budget identity constraint (27) yields the following system of inverse demand equations:

$$p_q(q) = \frac{\alpha_q + \beta_q \exp(u)}{1+\exp(u)} \frac{y - \sum_q p_q q}{q-\overline{q}}, \tag{28}$$

where p_q are "prices" - or in this case, the marginal valuation - of goods and services q and y is the economy's output per capita.

2.13 Welfare

The objective of the planner is to maximize welfare function, Ω, defined as the sum of net aggregate surplus discounted at the constant rate $\delta > 0$, and the bequest value of unmanaged and commercial forest areas.[11] Net surplus is computed by integrating the marginal valuation of each product, less the land access costs and non-land-based costs of producing each good. Thus, for agricultural output, food, and timber products, this represents non-land production costs.

[11] We do not consider the bequest value of protected forests, as they cannot be "scrapped" in our model.

For energy, these are non-land biofuels costs and fossil fuel costs. For fertilizers, these are non-energy costs. For forestry, these are harvesting and planting costs. And for recreation, these are the costs of maintaining natural parks. The planner allocates commercial land for agricultural product and timber production, and the scarce fossil fuels and reserved natural forest land to solve the following problem:

$$\max_{f,e,s,r} \Omega = \sum_{t=0}^{T-1} \delta^t \begin{bmatrix} \sum_{q=f,e,s,r,o} \int_0^{q^*} \left(p_q\left(q\right) - c_q\left(q\right)\right) dq \\ -c_t^N - c_t^R - c^\phi \phi_t - c^g g_t - c^p W_t^p - c_t^w \end{bmatrix} + \delta^T \Gamma\left(N_T^N, W_T\right) \tag{29}$$

s.t. constraints (1)-(28), where Γ is the scrap value function.

3 Model Baseline

This section describes the results of simulations of the model baseline. The baseline construction is documented in the technical appendix. We solve the model over the period 2005 - 2204, and present the results for the first 100 years to minimize the effect of terminal period conditions on our analysis.

Figure 1 depicts the optimal allocation of global land-use, GHG emissions, consumption of goods and services that draw on land resources, and consumption of biofuels in the model baseline. Beginning with the upper left-hand panel of Figure 1, we see that, in the short-run cropland area increases, reaching its maximum of 1.75 billion hectares in 2050 (14 percent larger compared to 2004), whereas managed forest area remains practically unchanged at 1.64 billion hectares (1 percent larger compared to 2004). In the medium- and long-run, slower population growth, rising real income and agricultural productivity, and energy efficiency improvements result in a decline in demand for cropland and an increase in demand for managed forests. By 2100 cropland area declines to 1.44 billion hectares (6 percent smaller compared to 2004), whereas managed forest area increases to 1.96 billion hectares (21 percent larger compared to 2004). Protected natural land area increases moderately in the short- to medium- run, and in 2050 amounts to 0.25 billion hectares (22 percent larger compared to 2004). In the long-run, the area of protected natural land increases sharply to 0.65 billion hectares in 2100 (216 percent larger compared to 2004), with most of the increase taking place after 2050.

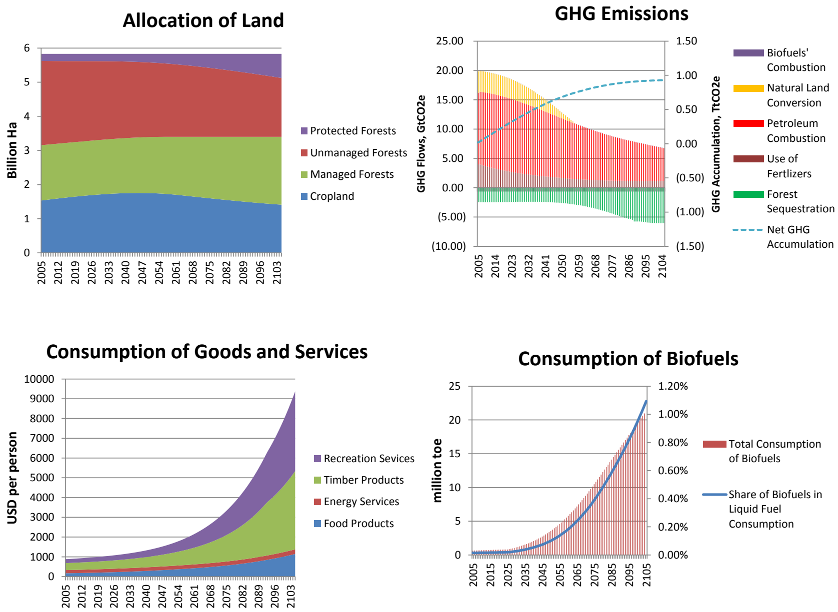

Figure 1: Model Baseline

The upper right-hand panel in Figure 1 reports gross GHG emissions flows and their net accumulation over time. Positive bars in this panel denote emissions, whereas negative bars denote carbon sequestration through forests.[12] Combustion of petroleum products is the major source of GHG emissions in the model, which amount to 13.5 GtCO_2e in 2004. In the long-run the demand for petroleum products declines due to higher oil prices and energy efficiency improvements, and GHG emissions from petroleum combustion decline by 52% relative to 2004, reaching 5.9 GtCO_2e in 2104. GHG emissions from conversion of natural land remain significant in short- run, and amount to 3.1 GtCO_2e in 2025 (10 percent smaller compared to 2004). In the medium run, increasing access costs of natural land combined with declining demand for commercial land, results in a sharp decline in deforestation. GHG emissions from deforestation decrease to 0.95 GtCO_2e in 2050 (72 percent smaller compared to 2004) and cease entirely by 2060, along this optimal global path of land use. GHG emis-

[12] A fraction of these GHG emissions flows is also sequestered by atmospheric and ocean sinks. We ignore this complication as our model does not provide comprehensive accounting of all GHG emissions flows, and focuses on understanding emissions from land use and related sectors.

sions from production and application of fertilizers decline steadily as prices of natural gas increase and pressure on croplands diminishes in the face of slowing global population growth and improving crop technology. In 2100, GHG emissions from production and application of fertilizers amount to 1.15 GtCO_2e (71 percent smaller compared to 2004). GHG emissions' sequestration from managed forests increases in the short run with the removal of older tree vintages and regrowth of new forest. In 2050 annual sequestration of GHG emissions by the global forestry sector amounts to 2.6 GtCO_2e (7.5 percent larger compared to 2004). In the medium-run and the long-run sequestered GHG emissions continue to increase faster with the increase in managed forest area. In 2100 sequestered GHG emissions amount to 6 GtCO_2e (147 percent larger compared to 2004). The gross emissions from biofuels' consumption (excluding indirect land use effects, which are reported separately) are quite modest, amounting to just 6 MtCO_2e in 2050 and 33.5 MtCO_2e in 2100. Overall, accumulated GHG flows grow rapidly, adding on average 13.6 GtCO_2e per annum in the first part of the century, reaching 0.68 TtCO_2e by 2050. Accumulation of GHG flows occurs at much slower rate (5 GtCO_2e per annum) in the second part of the century, reaching 0.93 TtCO_2e by 2100. As explained above, higher oil prices, improved energy efficiency, decline in deforestation and expanded forest sequestration are the main reasons for the slowdown in accumulation of GHG emissions.

The lower left-hand panel in Figure 1 illustrates the results for per-capita consumption of goods and services that draw on land resources. The consumption of all goods and services increases in absolute terms. The growth in per capita consumption is fueled by productivity growth across the board, while population growth declines over the baseline. In 2100 the per capita consumption of services from processed food, energy, processed timber, and recreation, are respectively higher by a factor of 6, 1.5, 10.5 and 20 compared to their levels in 2004. Of course, this does not translate into an equivalent increase in consumption of the bulk agriculture and timber products. Rather most of this rise in real consumption is due to efficiency gains in the processing sectors, as well as increases in the use of non-primary inputs in the production process. In relative terms, in 2100 the budget share of recreation services increases, budget shares of food and energy services decline, and the budget share of timber products remains relatively unchanged compared to their levels in 2004. This result is consistent with calibrated structure of AIDADS preferences.

The lower right-hand panel of Figure 1 describes the results for consumption of biofuels.[13] The consumption of biofuels grows in short-, medium-, and long-run as oil prices and agricultural yields increase. In 2100 the per capita consumption of biofuels is 20 Mtoe, considerably higher than in 2004, but still small in relative terms (0.95 percent of total consumption of liquid fuels).[14]

4 Counterfactual Scenarios

In practice, private and public land allocation decisions must be made despite significant uncertainty about the future productivity of land in different uses, as well as the future valuation of environmental services from this land, including biodiversity and carbon sequestration. This uncertainty is particularly problematic in light of the fact that some of the decisions are irreversible (e.g., cutting down natural forests, extraction and combustion of fossil fuels) and others take considerable time to reverse (e.g., harvesting a mature forest). Though we do not explicitly incorporate uncertainty in the model's optimization stage, we do examine the ways in which global land-use responds to changes in factors corresponding to the most important sources of uncertainty associated with this problem. These sources include (but are not limited to) variations in agricultural yield, θ^g, liquid fossil fuels' costs, p_x, and the future valuation of GHG abatement, expressed through the stringency of the GHG emissions constraint, $\bar{z}^L$.To do this, we utilize the model to simulate the effects of the following scenarios, each of which has the potential to put greater pressure on the world's land resources[15]:

[13] In our baseline, biofuels expansion is driven solely by oil prices. Of course there are government mandates which have played an important role in biofuel expansion in the US and the EU, in particular. However, in the long run, we believe that the fare of biofuels will be largely determined by oil prices. In our baseline, oil prices are rising steadily such that we expect the US mandates for first generation biofuels will not be binding (Meyer et al. 2011). More generally, we expect that budgetary pressures will limit the extent to which governments will be willing to subsidize biofuels in the coming decades. This leaves oil prices as the primary driver of biofuels expansion.

[14] These results are smaller compared to recent studies exploring the competition for land between biofuels and food production. For example, the refence case projections of Gurgel et al. (2007) predict that biofuels (including solid biomass used for electric power generation) should globally account for almost 17% of primary energy demand in 2100. Chakravorty et al.'s (2011) simulations show that, in the absence of regulation, the global share of petroleum in ground transportation steadily decreases from 95% in 2010 to 88% in 2050. These discrepancies can be explained by differences in modelling assumptions, including elasticity of energy demand, substitutability of biofuels and fossil fuels, energy efficiency projections, biofuels technology and production costs, and biofuels' end-use. We explore model sensitivities to these factors in technical appendix.

[15] We show the model sensitivity to changes in other important model parameters in technical appendix.

scenario A: the rate of growth agricultural yield permanently declines due to adverse effects of climate change;

scenario E: the rate of growth in liquid fossil fuel costs permanently increases because of rising extraction costs and (or) more stringent climate policies, aimed specifically at fossil fuels[16];

scenario T: the land based GHG emissions constraint is introduced, and becomes more stringent over time, as land-use climate mitigation strategies become more aggressive;

We also consider the combinations of scenarios A and E (scenario AE) and scenarios A, E, and T (scenario AET).

We assume that all of these alternative scenarios are realized after 20 years from the 2005 starting period, i.e. 2025. We assume that the above mentioned "events" are fully anticipated, and simulate the model for the entire time horizon, focusing our analysis on the next 100 years. The construction of counterfactual scenarios is documented in technical appendix.

4.1 Results of Counterfactual Scenarios

Figures 2, 3, and 4 describe the results of simulations of changes in the optimal allocation of global land-use, GHG emissions, consumption of goods and services that draw on land resources, and consumption of biofuels for scenarios A, AE, and AET. For scenario A, we report changes, which are incremental to the model baseline. For scenario AE, we report incremental changes to scenario A. For scenario AET, we report incremental changes to scenario AE. The results for scenarios E and T are not described in this section, as they are numerically close to reported incremental changes for scenarios AE and AET. We show the results for scenarios E and T in the technical appendix.

4.1.1 Scenario A: Declining Growth of Agricultural Yield

Figure 2 describes the results of simulations of changes relative to the model baseline for the counterfactual scenario A corresponding to the gradual decline in the rate of growth of agricultural yield starting in 2025. The upper left-hand panel in Figure 2 shows the results for changes in allocation of land use relative to the baseline scenario. Declining agricultural productivity results in greater

[16] There are also a number of factors contributing to a potential decline in highly uncertain fossil fuel costs (e.g. greater penetration of compressed natural gas and renewable electricity in transportation sector). Our choice of rising fossil fuel costs in this scenario is motivated by understanding global land use decisions under greater resource scarcity.

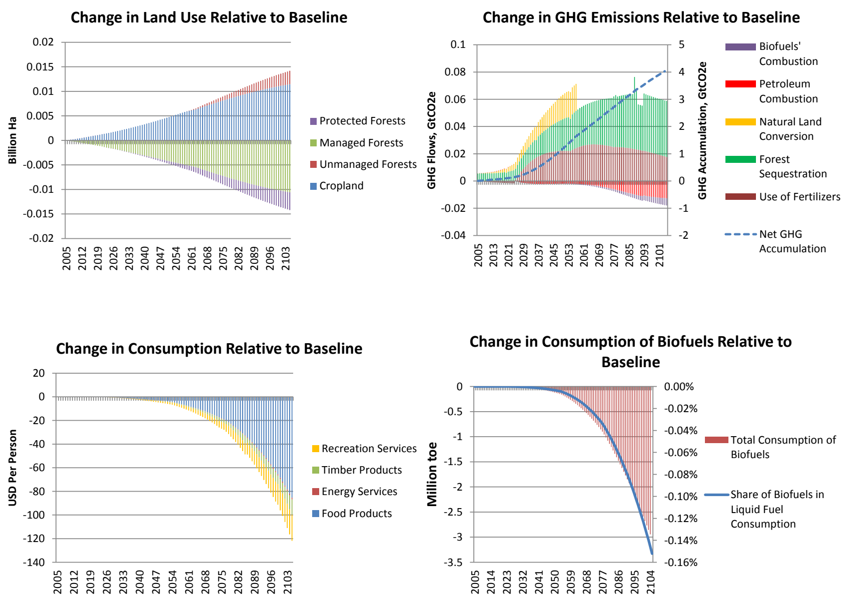

Figure 2: Scenario A: Declining Agricultural Yield

requirements for cropland and fertilizers to produce agricultural output used in production of food and energy services. However, the expansion of cropland is relatively small. Compared to the baseline scenario, the cropland area expands further by 4.5 million hectares (0.25 percent) in 2050 and by 11 million hectares (0.75 percent) in 2100. Managed forest area declines by 4 million hectares in 2050 and by 10 million hectares in 2100. In addition, protected forest area declines by 0.5 million hectares in 2050 and by 3 million hectares in 2100. Modest increase in use of cropland relative to the baseline scenario is explained by a significant decline in agricultural output and an increased use of fertilizers. In 2100 the production of agricultural output falls by 46 million tons (7 percent), whereas application of fertilizers increases by 13 million tons (2 percent).

The upper right-hand panel in Figure 2 shows the results for changes in GHG emissions relative to the baseline scenario. The effect of declining agricultural productivity results in an increase in GHG emissions from more use of fertilizers, natural land conversion, and reduced forest sequestration. In the short- and medium- run, the increase in GHG emissions comes from the natural land conversion, which occurs in response to an anticipated decline in agricultural yield. In 2050 the GHG emissions from the natural land conversion are 18 $MtCO_2e$ (2 percent) larger relative to the baseline scenario. In the medium- and long-run the increase in GHG emissions also comes from expansion in fertilizers' use and reduced forest sequestration. Compared to the baseline scenario, the GHG emissions from fertilizers' use and forest sequestration increase by 22 and 23 $MtCO_2e$ in 2050, and by 20 and 41 $MtCO_2e$ (2 and 1 percent) in 2100. There is also a small decline in long run GHG emissions from the reduced demand for energy services. Overall, accumulated GHG emissions increase modestly relative to the baseline scenario, reaching 4 $GtCO_2e$ by 2100.

The lower left-hand panel in Figure 2 shows the results for changes in per-capita consumption of goods and services that draw on land resources. Compared to the baseline scenario consumption of all goods and services decreases. There is a significant decline in the consumption of processed food services. In 2100 their per capita consumption is about 7 percent lower than in the baseline scenario. The reduction in consumption of services of energy, timber products, and recreation is small. Compared to the baseline scenario they decline by less than 1 percent.

The lower right-hand panel in Figure 2 shows the results for changes in biofuels. Declining agricultural productivity depresses production of biofuels. In 2100 the total consumption of biofuels decreases by 2.6 million toe (13 percent) compared to the baseline scenario. The share of biofuels in liquid fuel consumption declines, and amounts to 0.8 percent of total liquid fuel consumption in 2100.

4.1.2 Scenario AE: Declining Growth of Agricultural Yield *and* Rising Fossil Fuel Costs

Figure 3 describes the results of simulations of changes for the counterfactual scenario AE relative to scenario A. This adds the effect of permanent increase in the rate of growth in liquid fossil fuel costs to the effect of a permanent decline in the rate of growth of agricultural yield starting in 2025. The upper left-hand panel in Figure 3 shows the results for changes in allocation of land use *relative to scenario A*. Rising oil and natural gas prices increase the costs of fertilizers and petroleum consumption. As biofuels substitute for fossil fuels in demand for energy services, the demand for biofuels increases. This, in turn, increases the demand for cropland needed to produce the feedstock. Cropland requirements also rise due to the increased cost of fertilizer – a key ingredient

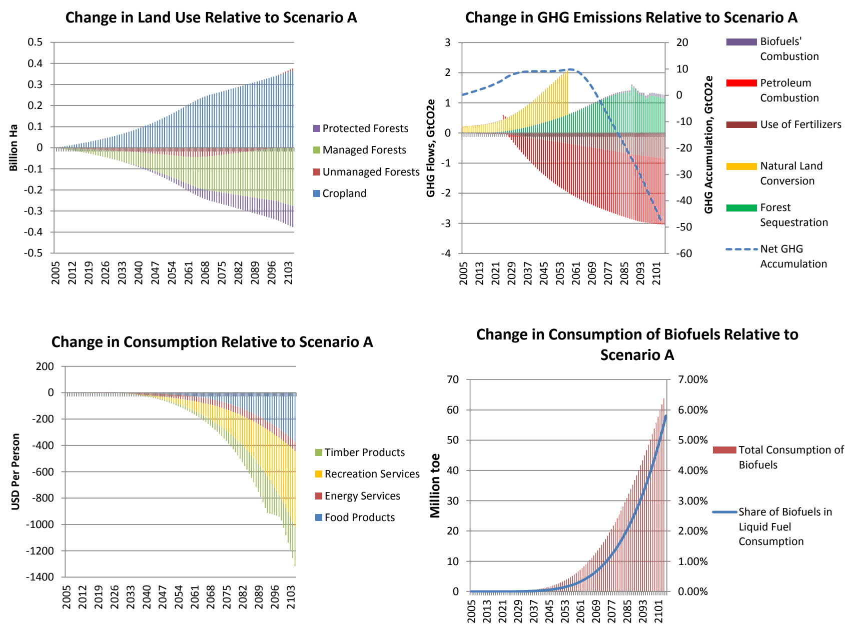

Figure 3: Scenario AE: Declining Agricultural Yield and Rising Fossil Fuel Costs

in the intensification of agricultural production. Compared to scenario A, the cropland area expands by additional 138 million hectares (8 percent) in 2050. The expansion of cropland comes at the expense of forest area. Managed forest area declines by 91 million hectares (5.5 percent), and the unmanaged and protected forest areas decline by respectively 32 and 15 million hectares (1.5 and 6 percent). In the long run, the cropland area continues to expand, adding 347 million hectares (24 percent) more relative to scenario A in 2100. Managed and protected forests continue to decline in the long-run, losing additional 259, and 92 million hectares (13 and 14 percent), whereas unmanaged forest area increases by 4 million hectares (less than 1 percent) relative to scenario A in 2100.[17]

The upper right-hand panel in Figure 3 shows the results for changes in GHG emissions. Preceding the anticipated increase in energy prices the increase GHG emissions comes mainly from deforestation, caused by conversion of natural and

[17] While these numbers are large they are not inconsistent with findings of other studies. For example, the results of simulations based on MIT EPPA model (Gurgel et al. 2007) suggest cropland expansion around 420-470 million Ha for bioenergy production by 2050 in the reference case. Chakravorty et al.'s (2011) model predicts the area about 150 million Ha is cleared in the medium-income countries by 2025 in the reference case scenario.

managed forest areas to cropland. In 2025 the GHG emissions from natural land conversion increase by 0.41 $GtCO_2e$ (13 percent) compared to scenario A. In the medium run, GHG emissions from deforestation continue to increase, whereas GHG emissions from petroleum products and fertilizer consumption decline. In 2050 the GHG emission flows from natural land conversion and reduced forest sequestration increase by 1.23 and 0.45 $GtCO_2e$ (122 and 17 percent) compared to scenario A. GHG emissions from petroleum combustion, and fertilizers' use reduce by 1.37, and 0.28 $GtCO_2e$ (13.5 and 16 percent) compared to baseline scenario. In the long run, as natural land conversion ceases, the increase in GHG comes from reduced forest sequestration and combustion of biofuels. In 2100 these emissions account for an additional 1.22 $GtCO_2e$ and 96 $MtCO_2e$ (20 and 329 percent) compared to scenario A. GHG emissions from combustion of petroleum products, and fertilizers' production and application fall by 2.2 and 0.8 $GtCO_2e$ (37 and 68 percent) compared to scenario A. Overall, compared to scenario A accumulated GHG emissions increase in the short and the medium term, reaching their maximum of 9.6 $GtCO_2e$ in 2060. In the long run, the GHG emissions reductions from fertilizers' use and combustion of petroleum products outweigh the GHG emissions increase from reduced forest sequestration and combustion of biofuels. Compared to scenario A, accumulated GHG emissions decline by 41 $GtCO_2e$ in 2100.

The lower left-hand panel in Figure 3 shows the results for changes in per-capita consumption of goods and services that draw on land resources. Compared to scenario A consumption of all land-based goods and services decrease. In 2100 the most significant decline is in consumption of services from processed food products and energy. Consumption of both declines by 31 percent, compared to scenario A. Consumption of recreation services falls by 14%, whereas the consumption of services of timber products decreases by 5.5% compared to scenario A.

The lower right-hand panel in Figure 3 shows the results for changes in biofuels. Higher oil prices increase the demand for biofuels, and by 2100 their total consumption increases drastically by additional 55 million toe (329 percent) compared to scenario A. The share of biofuels in liquid fuel consumption raises significantly, and accounts to 5.5 percent of total liquid fuel consumption.

4.1.3 Scenario AET: Declining Growth of Agricultural Yield *and* Rising Fossil Fuel Costs *and* Land-Use Emissions Target

Figure 4 describes the results of simulations of changes relative to scenario AE for the counterfactual scenario AET. This figure illustrates the effect of adding the land-use GHG emissions constraint to the effects of a permanent increase in the rate of growth in liquid fossil fuel costs and permanent decline in the rate of growth of agricultural yield to starting in 2025. The upper left-hand panel in Figure 4 shows the results for changes in allocation of land use relative to scenario AE. Introduction of a land-use GHG emissions constraint has an intertemporal effect on allocation of global land use. As natural forest land conversion to agricultural land is the main short-term driver of GHG emissions from land-use, further expansion of agricultural land becomes more difficult after the GHG constraint is introduced. Therefore, in anticipation of GHG emissions target, there is a short-term increase in demand for conversion of natural forest land. Compared to scenario AE, the cropland area expands by additional 8 million hectares (0.5 percent) in 2025. The demand for managed forest land also increases, as imposition of GHG emissions constraint requires greater sequestration by managed forests.

In 2025 managed forest area expands by 29 million hectares (2 percent). The expansion of agricultural and managed forest area puts greater pressure on natural lands. Unmanaged and protected forest areas decline by respectively 32 and 5 million hectares (1 and 2 percent) in 2025. In the medium- and long-run, as the GHG emissions target becomes more stringent, there an increase in managed forest area used for GHG sequestration. Compared to scenario AE, the managed forest area expands further by 52 million hectares (3 percent) in 2050 and by 131 million hectares (7.5 percent) in 2100. Most of the increase in the managed forest area is compensated by the reduction in cropland. The cropland area declines by 69 million hectares (3.5 percent) in 2050 and by 157 million hectares (8.5 percent) 2100. Natural land conversion declines in relative terms after 2025. Compared to scenario AE, unmanaged forest area increases by 29.5 million hectares (1.5 percent) in 2100.

The upper right-hand panel in Figure 4 shows the results for changes in gross GHG emissions. Preceding the introduction of the GHG emissions constraint, there is a large increase in GHG emissions, which increases the GHG emissions stock and significantly reduces the effectiveness of the target. Two factors contribute to this increase. First, there is an increased conversion of natural forest

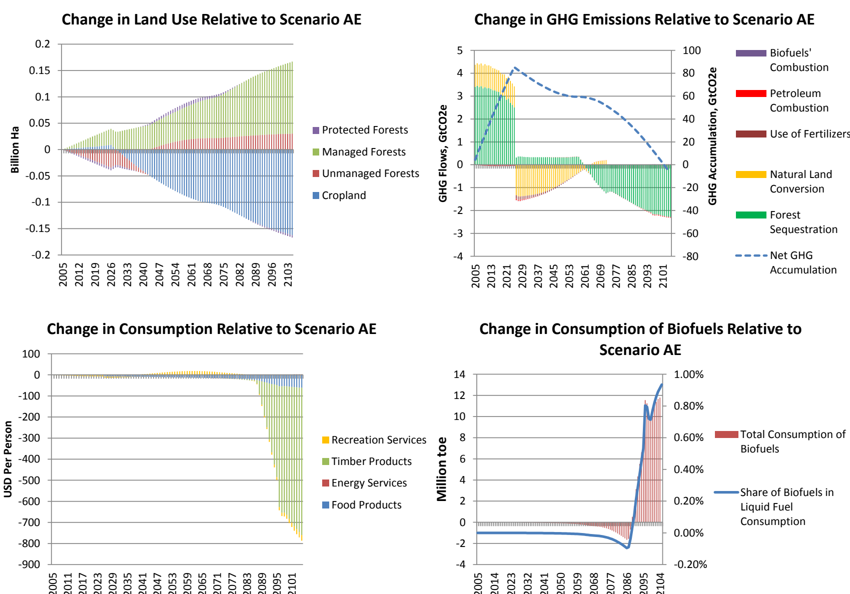

Figure 4: Scenario AET: Declining Growth of Agricultural Yield *and* Rising Fossil Fuel Costs *and* Land-Use Emissions Target

lands. Second, GHG sequestration by managed forests decline, driven by the change in the vintage structure of managed forests. In 2025 the GHG emissions from natural land conversion and reduced forest sequestration increase by 0.92 and 2.5 $GtCO_2e$ (26 and 106 percent) compared to scenario AE. After the introduction of the GHG emissions constraint, the GHG emissions from land use decline. In the medium run, the main source of reduction in GHG emission is due to decline in natural land conversion, which amounts to 0.83 $GtCO_2e$ (35 percent) in 2050, compared to scenario AE. In the long-run, increased GHG sequestration by managed forests is the main factor contributing to the reduction in GHG emissions. Compared to scenario AE, the reduction in GHG emissions due to increased forest sequestration amounts to 2.2 $GtCO_2e$ (46 percent) in 2100. Introduction of GHG target also results in a modest decline of consumption of petroleum products and fertilizers, and a modest increase in consumption of biofuels. The GHG emissions from petroleum combustion and fertilizers' use decline by 27 and 20 $MtCO_2e$ (0.7 and 5 percent) in 2100. The GHG emissions from biofuels combustion increase by 18 $MtCO_2e$ (14 percent) in 2100.

Overall, in the presence of intertemporal substitution, the land based GHG emissions target appears to be ineffective over the 100 year time horizon. Preceding the introduction of the constraint, cumulative GHG emissions increase by 85.2 $GtCO_2e$. After the introduction of the constraint, the GHG emissions from land use cumulatively decline by 81.5 $GtCO_2e$. The resulting intertemporal leakage (the ratio of cumulative increase in GHG emissions preceding the GHG target to cumulative decline after the GHG target) is 105 percent.[18] This finding is consistent with the theory of "green paradox", which originates from intertemporal models analyzing climate policy effects on the optimal path of fossil fuel extraction (Sinn 2008, Eichner and Pethig 2011).

The lower left-hand panel in Figure 4 shows the results for changes in per-capita consumption of goods and services that draw on land resources. Compared to scenario AE consumption of all goods and services does not change much in the short- and the medium-run. In the long run, there is a significant decline in consumption of services from processed food and timber. In 2100 they decline by 8 and 19 percent compared to scenario AE. The expansion of biofuels sector leads to the growth in consumption of energy services, which increase by 1 percent in 2100, as compared to scenario AE. The consumption of recreation services declines modestly by 0.5 percent.

[18] The size of intertemporal leakage is reduced to 27 percent over the period of 200 years.

The lower right-hand panel in Figure 4 shows the results for changes in biofuels. Introduction of GHG emissions constraint favours the displacement of petroleum products for biofuels. This effect is small in the short- and medium-run. However, in the long run there is a significant increase in the consumption of biofuels. In 2100 the total consumption of biofuels increases by additional 10 million toe (14 percent) compared to scenario AE. The share of biofuels in liquid fuel consumption also raises, and accounts to 6 percent of total liquid fuel consumption.

5 Conclusions

We analyze the optimal allocation of the world's land resources over the course of the next century in the unified economic framework, which integrates five, rather distinct strands of literature into a single, intertemporally consistent, analytical model at global scale. This long-run, forward-looking partial equilibrium model covers key sectors drawing on the world's land resources, and incorporates growing demands for food, renewable energy, and forest products, and increasing non-market demands for ecosystem services. We also consider alternative GHG constraints, as well as the potential impacts of climate change itself on the productivity of land in agriculture, forestry and ecosystem services.

Our baseline accurately reflects developments in global land use over the 10 years that have already transpired, while also incorporating long-run projections of population, income and demand growth from a variety of international agencies. The model baseline demonstrates that, in the absence of market imperfections, deforestation associated with cropland expansion, which accounts for a large share of land-use GHG emission, declines along the optimal land-use trajectory in the medium run. In the long-run there is a significant expansion of the forestry sector, and the area of protected natural lands, which deliver eco-system services, increases drastically. While the consumption of biofuels increases rapidly in the long-run, its share in gross liquid fuel consumption remains insignificant.

We then consider three counterfactual scenarios for changes in factors corresponding to the most important sources of uncertainty associated with this problem: energy prices, agricultural productivity, and global GHG emissions regulations. Though adverse productivity shocks from climate change have a modest effect on global land use, consumption of agricultural output declines significantly in the long-run. Energy prices and policies have a significant effect on the optimal deforestation rate and on the overall amount of land used in agriculture. In the long-run, cropland area increases drastically, and substantial deforestation occurs. The GHG emissions from land use also increase significantly, offsetting the emissions fall from reduced petroleum consumption. When we also expect the world's land base to deliver land-based GHG abatement, the pressure on global natural land resources becomes even more significant. While the introduction of the land based GHG emissions constraint leads to a significant reduction in GHG emission flows over the term of hundred years, its effectiveness is eroded by an even greater increase in GHG emissions before such constraint is introduced.

In further work it will be interesting to extend the scope of this study by exploring the model's sensitivity to other important uncertainty sources, such as the economywide TFP and biofuel production technology, as well as explicitly incorporating uncertainty in the model's optimization stage.

References

Antoine, B., Gurgel, A. and Reilly, J.: 2008, Will Recreation Demand for Land Limit Biofuels Production?, *Journal of Agricultural & Food Industrial Organization* **6**(2), 5.

Babiker, M., Gurgel, A., Paltsev, S. and Reilly, J.: 2009, Forward-looking versus Recursive-dynamic Modeling in Climate Policy Analysis: A Comparison, *Economic Modelling* **26**(6), 1341–1354.

Bulte, E., van Soest, D., Van Kooten, G. and Schipper, R.: 2002, Forest Conservation in Costa Rica when Nonuse Benefits are Uncertain but Rising, *American Journal of Agricultural Economics* **84**(1), 150–160.

Burney, J., Davis, S. and Lobell, D.: 2010, Greenhouse Gas Mitigation by Agricultural Intensification, *Proceedings of the National Academy of Sciences* **107**(26), 12052–12057.

Chakravorty, U., Hubert, M., Moreaux, M. and Nostbakken, L.: 2011, Will Biofuel Mandates Raise Food Prices?, *Working Paper 2011-01*, Department of Economics, University of Alberta.

Chakravorty, U., Magné, B. and Moreaux, M.: 2008, A Dynamic Model of Food and Clean Energy, *Journal of Economic Dynamics and Control* **32**(4), 1181–1203.

Chen, X., Huang, H., Khanna, M. and Önal, H.: 2011, Meeting the Mandate for Biofuels: Implications for Land Use, Food and Fuel Prices, *Working Paper 16697*, National Bureau of Economic Research.

Choi, S., Ohrel, S. and Sohngen, B.: 2011a, Extending the GTAP Family of Models: A Partial Equilibrium Approach to Measuring the Costs of Carbon Sequestration and Avoided Deforestation, Selected Paper Prepared for Presentation at the GTAP 2011 Annual Meeting Venice, Italy.

Choi, S., Sohngen, B., Rose, S., Hertel, T. and Golub, A.: 2011b, Total Factor Productivity Change in Agriculture and Emissions from Deforestation, *American Journal of Agricultural Economics* **93**(2), 349 –355.

Conrad, J.: 1997, On the Option Value of Old-growth Forest, *Ecological Economics* **22**(2), 97–102.

Conrad, J.: 2000, Wilderness: Options to Preserve, Extract, or Develop, *Resource and Energy Economics* **22**(3), 205–219.

Cranfield, J., Eales, J., Hertel, T. and Preckel, P.: 2003, Model Selection when Estimating and Predicting Consumer Demands using International, Cross Section Data, *Empirical Economics* **28**(2), 353–364.

Deaton, A. and Muellbauer, J.: 1980, An Almost Ideal Demand System, *The American Economic Review* **70**(3), 312–326.

Eichner, T. and Pethig, R.: 2011, Carbon Leakage, the Green Paradox and Perfect Future Markets, *International Economic Review* **52**(3), 767–805.

Fearnside, P.: 2000, Global Warming and Tropical Land-use Change: Greenhouse Gas Emissions from Biomass Burning, Decomposition and Soils in Forest Conversion, Shifting Cultivation and Secondary Vegetation, *Climatic Change* **46**(1), 115–158.

Gillingham, K., Smith, S. and Sands, R.: 2008, Impact of Bioenergy Crops in a Carbon Dioxide Constrained World: an Application of the MiniCAM Energy-Agriculture and Land Use Model, *Mitigation and Adaptation Strategies for Global Change* **13**(7), 675–701.

Golub, A., Hertel, T. and Sohngen, B.: 2009, Land Use Modeling in Recursively-Dynamic GTAP Framework, *in* T. Hertel, S. Rose and R. Tol (eds), *Economic Analysis of Land Use in Global Climate Change Policy*, Routledge, pp. 235–278.

Gurgel, A., Cronin, T., Reilly, J., Paltsev, S., Kicklighter, D. and Melillo, J.: 2011, Food, Fuel, Forests and the Pricing of Ecosystem Services, *American Journal of Agricultural Economics* **92**(2), 342–348.

Gurgel, A., Reilly, J. and Paltsev, S.: 2007, Potential Land Use Implications of a Global Biofuels Industry, *Journal of Agricultural & Food Industrial Organization* **5**(2), 1–34.

Hanoch, G.: 1975, Production and Demand Models with Direct or Indirect Implicit Additivity, *Econometrica* **43**(3), 395–419.

Houghton, R.: 2003, Revised Estimates of the Annual Net Flux of Carbon to the Atmosphere from Changes in Land Use and Land Management 1850–2000, *Tellus B* **55**(2), 378–390.

Ianchovichina, E., Darwin, R. and Shoemaker, R.: 2001, Resource Use and Technological Progress in Agriculture: a Dynamic General Equilibrium Analysis, *Ecological Economics* **38**(2), 275–291.

Leroux, A., Martin, V. and Goeschl, T.: 2009, Optimal Conservation, Extinction Debt, and the Augmented Quasi-option Value, *Journal of Environmental Economics and Management* **58**(1), 43–57.

Meyer, S., Binfield, J., Westhoff, P. and Thompson, W.: 2011, U.S. Biofuels Baseline: The Impact of Extending the $0.45 Ethanol Blenders Credit, *FAPRI-MU Report 07-11*, Food and Agricultural Policy Research Institute at the University of Missouri-Columbia.

Richards, K. and Stokes, C.: 2004, A Review of Forest Carbon Sequestration Cost Studies: A Dozen Years of Research, *Climatic Change* **63**(1), 1–48.

Rimmer, M. and Powell, A.: 1996, An Implicitly Additive Demand System, *Applied Economics* **28**(12), 1613–1622.

Searchinger, T., Heimlich, R., Houghton, R., Dong, F., Elobeid, A., Fabiosa, J., Tokgoz, S., Hayes, D. and Yu, T.: 2008, Use of US Croplands for Biofuels

Increases Greenhouse Gases through Emissions from Land-Use Change, *Science* **319**(5867), 1238.

Sinn, H.: 2008, Public Policies Against Global Warming: a Supply Side Approach, *International Tax and Public Finance* **15**(4), 360–394.

Sohngen, B. and Mendelsohn, R.: 2003, An Optimal Control Model of Forest Carbon Sequestration, *American Journal of Agricultural Economics* **85**(2), 448–457.

Sohngen, B. and Mendelsohn, R.: 2007, A Sensitivity Analysis of Forest Carbon Sequestration, *in* M. Schlesinger (ed.), *Human-Induced Climate Change: An Interdisciplinary Assessment*, Cambridge University Press, pp. 227–237.

Sorrell, S. and Dimitropoulos, J.: 2008, The Rebound Effect: Microeconomic Definitions, Limitations and Extensions, *Ecological Economics* **65**(3), 636–649.

Stavins, R.: 1999, The Costs of Carbon Sequestration: A Revealed-preference Approach, *The American Economic Review* **89**(4), 994–1009.

Wise, M., Calvin, K., Thomson, A., Clarke, L., Bond-Lamberty, B., Sands, R., Smith, S., Janetos, A. and Edmonds, J.: 2009, Implications of Limiting CO2 Concentrations for Land Use and Energy, *Science* **324**(5931), 1183.

Yu, W., Hertel, T., Preckel, P. and Eales, J.: 2004, Projecting World Food Demand Using Alternative Demand Systems, *Economic Modelling* **21**(1), 99–129.